PHYSICAL REVIEW VOLUME 134, NUMBER 5A 1 JUNE 1964

Ionization and Dissociation of Fast H_2 Molecules Incident on H_2 Gas*

G. W. McClure
Sandia Laboratory, Alburquerque, New Mexico
(Received 9 January 1964)

The yield cross sections $\sigma_{H_2^+}$, σ_{H^+}, and σ_H for production of fast H_2^+ and H^+ ions and H atoms resulting from the ionization and dissociation of fast H_2 molecules in single collisions with H_2 gas molecules have been measured in the 6- to 120-keV energy range (collision velocity 0.7 to 3.2×10^8 cm/sec). The neutral primary beam contained a fraction of H atoms which was determined by proportional counter analysis. Secondary particles produced by the H atoms in the primary beam were determined in separate H beam experiments and subtracted from the composite (H,H_2) neutral beam data to yield the production of secondaries due to H_2 primaries alone. Cross section $\sigma_{H_2^+}$ increases monatonically from 0.5 to 2.0 Å^2 in the energy range 6 to 120 keV while σ_{H^+} increases from 0.28 Å^2 at 7.5 keV to a maximum of 0.70 Å^2 at 50 keV. Cross section σ_H, measured only at 10 keV, was found to have an approximate value of 2.5 Å^2 based on an assumed shape of the H atom angular distribution at small angles. The results are compared with data on a number of collision processes in the same velocity range involving various species of hydrogen ions and H atoms incident on H_2 gas molecules.

INTRODUCTION

THERE is a growing need for experimental data concerning ionization and charge exchange in collisions of atomic particles at relative velocities of the order of 10^8 cm/sec. Such velocities are encountered in fusion machines, ionic propulsion engines, high-voltage gaseous dischanges, and nuclear explosions. Experiments with hydrogen ions and molecules are directly applicable to all of these problems and are needed as a guide to further development of collision theory. In the particular velocity range of interest, theoretical calculations of collision cross sections are most difficult because the optical electron velocity of the colliding particles is about the same as the atomic translational velocity. Neither the adiabatic nor the impulsive model of a collision is valid under these circumstances.

The main purpose of this paper is to report measurements of the cross sections for ionization and dissociation of 6- to 120-keV H_2 molecules in collision with H_2 gas molecules. Apparatus used previously for the study of H^+, H_2^+, and H_3^+ collisions with H_2 molecules was employed.[1] The method consists of preparing a monoenergetic beam of fast molecules by charge exchange, passing the beam through a thin target of H_2 gas and measuring the production of fast H^+ and H_2^+ ions and H neutral atoms.

The reactions contributing to the production of the observed species are as follows, neglecting reactions in which negative ions are formed.

Reaction 1: $H_2+H_2\rightarrow H+H+(H_2)$,

Reaction 2: $H_2+H_2\rightarrow H_2^++(e+H_2)$,

Reaction 3: $H_2+H_2\rightarrow H^++H+(e+H_2)$,

Reaction 4: $H_2+H_2\rightarrow H^++H^++(e+e+H_2)$.

Here the heavy fragments of the primary H_2 molecules are shown immediately following the arrow while electrons removed from the primary and the post-collision target molecule are shown in parentheses on the right. The target H_2 molecules may be ionized, excited or dissociated, and the product particles H_2^+ and H may carry off some energy in the form of internal excitation, but in the great majority of collisions of the type considered the two constituent protons of the primary molecules, whether bound or dissociated after the collision, suffer very little change of velocity or direction of motion.

The present measurements do not completely resolve the above reactions but rather determine the yield cross sections σ_{H^+}, $\sigma_{H_2^+}$, and σ_H for the three types of fast heavy particles H^+, H_2^+, and H. In terms of the reaction cross sections σ_1, σ_2, σ_3, σ_4 for the above reactions, the measured quantities are:

$$\sigma_{H_2^+}=\sigma_2,$$
$$\sigma_{H^+}=\sigma_3+2\sigma_4,$$
$$\sigma_H=2\sigma_1+\sigma_3.$$

Particle counting was used to measure the intensities of both the primary neutral beams and the secondary ion and neutral beams. The counter employed permitted H_2 and H neutrals of the same velocity to be clearly distinguished by the relative size of electrical impulses they produced. Ability of the counting system to resolve H and H_2 counts placed a lower limit of about 3 keV on the present method of measurement. The narrow slit aperture on the proportional counter (needed to support a thin-film gas barrier) prevented our use of a technique devised by Sweetman[2] which might otherwise have been employed to distinguish the reactions 1 to 4.

The apparatus was designed so that all heavy fragments of the primary molecule having a post-collision angle less than 2.2 deg relative to the direction of the H_2 beam could be detected. At the 6-keV lower energy limit of the present (H_2+H_2) measurements the cross section for Coulomb scattering through an angle greater

* This work performed under the auspices of the U. S. Atomic Energy Commission.

[1] G. W. McClure, Phys. Rev. **130**, 1852 (1963).

[2] D. R. Sweetman, Proc. Roy. Soc. (London) **A256**, 416 (1960).

than 2.2 deg of one of the two protons of the incident molecule against one of the two protons of the target molecule is 2×10^{-17} cm^2, neglecting screening. This cross section is of the same order of magnitude as the measured H^+ production cross section at 6 keV; hence, some error may be introduced into the H^+ data at this energy. However, throughout most of the present energy range no significant large angle scattering errors are expected due to Coulomb interactions.

At angles up to a few degrees from the forward direction the differential cross section for production of dissociation fragments of fast molecules may exceed that due to Coulomb scattering because of electronic transitions of the incident particle to antibonding states in which the two nuclei repel each other. Resulting production of dissociation fragments at angles outside the detector aperture may cause the measured cross sections to be 10 to 20% below the true total cross section at the lowest energies.

An important problem associated with the present measurements was that of producing a primary beam of neutral H_2 molecules. This was accomplished via the H_2^+ on H_2 reactions, studied previously,[1,2] which give rise to a mixed beam of H_2 molecules and H atoms of the same velocity via the processes

$$\text{Reaction 5:}\quad \mathbf{H_2^+}+H_2\rightarrow \mathbf{H_2}+(H_2^+),$$

$$\text{Reaction 6:}\quad \mathbf{H_2^+}+H_2\rightarrow \mathbf{H}+\mathbf{H}+(H_2^+),$$

$$\text{Reaction 7:}\quad \mathbf{H_2^+}+H_2\rightarrow \mathbf{H}+\mathbf{H^+}+(H_2).$$

In order to calculate the background production of H^+ caused by electron loss from the H atoms in the mixed neutral beam, it was necessary to know the cross section $\sigma_{0,1}$ for the reaction

$$\text{Reaction 8:}\quad \mathbf{H}+H_2\rightarrow \mathbf{H^+}+(e+H_2).$$

Although this cross section has been measured,[3–9] a serious discrepancy existed between the available measurements below 10 keV. Therefore, $\sigma_{0,1}$ was remeasured over the entire energy range 2 to 120 keV. At the same time, remeasurements of $\sigma_{0,-1}$, the cross section for the reaction

$$\text{Reaction 9:}\quad \mathbf{H}+H_2\rightarrow \mathbf{H^-}+(H_2^+)$$

were made to resolve a gross discrepancy in previous data on this process. Both measurements involving H atom primaries are discussed in the first portion of the section entitled Results. The second portion of the Results section deals with the (H_2+H_2) measurements.

All cross sections were measured relative to the cross section $\sigma_{1,0}$ for the reaction

$$\text{Reaction 10:}\quad \mathbf{H^+}+H_2\rightarrow \mathbf{H}+(H_2^+).$$

This reaction[10] serves as an excellent basis for calibration of collision experiments of the present type because (1) no excited states are possible in the incident proton beam, (2) the angular distribution of the product H atoms is very strongly peaked in the forward direction, and (3) the absolute value of the cross section has been measured in the neighborhood of 10–100 keV by a number of investigators whose results are in excellent agreement.

A major problem in the interpretation of any experiment using fast neutral beams produced by charge exchange is that of uncertainty concerning the quantum states of the incident particles. In the present work this question is not settled; however, a discussion of the possible states of excitation of the neutral particles is given. Also, the conditions of production of the neutral beams are fairly well defined so that future data on the initial population and decay of excited states produced in charge-exchange collisions may be brought to bear on a more refined interpretation of the present work.

The section entitled Discussion compares the (H_2+H_2) collision data, obtained for the first time in this investigation, with data on related collision processes.

APPARATUS

The ion source, ion accelerator, and magnetic beam analyzer described in Ref. 1 were used without alteration to provide a 1–20-keV beam of either H^+ or H_2^+ ions having an energy spread of approximately one percent. Either of these beams could be directed along the sequence of apertures S_1, S_2, S_3, and S_4 (Fig. 1) which formed the entrance and exit slits of two differentially pumped chambers T_1 and T_2 operated with separate gas controls and pressure gages. These chambers served as a neutralizing chamber and main collision chamber, respectively. Electrostatic deflection plates D_1 located between T_1 and T_2 were used in the neutral beam experiments to deflect unconverted ions emergent from T_1 out of the neutral beam, permitting only neutrals to enter T_2. To change from an ion beam experiment to a neutral beam experiment required only the closing of a bypass valve between T_1 and the main vacuum chamber, the admission of a gas to the neutralizing chamber T_1, and the application of a deflection voltage to plates D_1.

A second set of electrostatic deflection plates D_2 at the

---

[3] J. H. Montague, Phys. Rev. **81**, 1026 (1951).
[4] P. M. Stier and C. F. Barnett, Phys. Rev. **103**, 896 (1956).
[5] C. F. Barnett and H. K. Reynolds, Phys. Rev. **109**, 355 (1958).
[6] I. M. Fogel, V. A. Ankudinov, D. V. Pilipenko, and N. V. Topolia, Zh. Eksperim. i Teor. Fiz. **34**, 579 (1958) [English transl.: Soviet Phys.—JETP **7**, 400 (1958)].
[7] D. V. Pilipenko and I. M. Fogel, Zh. Eksperim. i Teor. Fiz. **42**, 936 (1962) [English transl.: Soviet Phys.—JETP **15**, 646 (1962)]. Data on $\sigma_{0,1}$ from this reference (9–30 keV) agree with data from Ref. 6.
[8] R. Curran and T. M. Donahue, Phys. Rev. **118**, 1233 (1960).
[9] Fred Schwirtzke, Z. Physik **157**, 510 (1960).

[10] S. K. Allison and M. Garcia Munoz, in *Atomic and Molecular Processes*, edited by D. R. Bates (Academic Press Inc., New York, 1962), p. 751.

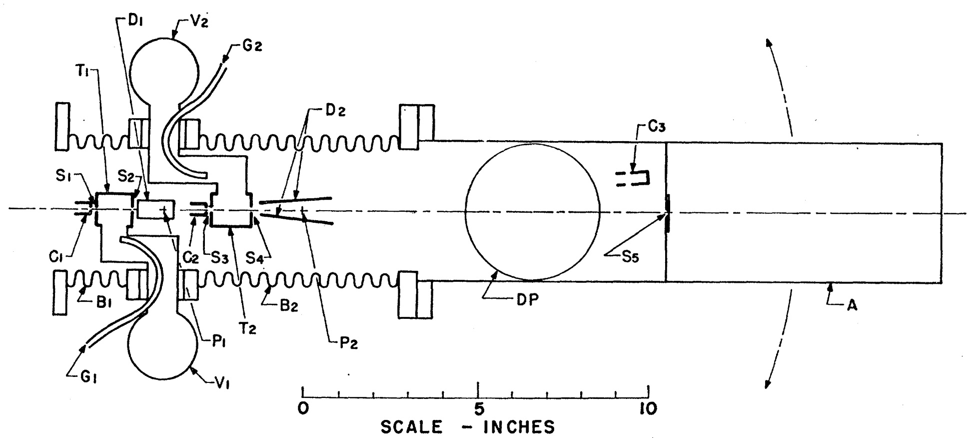

FIG. 1. Apparatus diagram. T_1 and T_2, collision chambers. V_1 and V_2, ionization gauges. G_1 and G_2, gas inlets. C_1, C_2, and C_3, Faraday cups. D_1 and D_2, deflection plates for deflecting charged particle beams off the main beam axis. S_1, S_2, S_3, and S_4, circular apertures having diameters 0.01, 0.02, 0.01, and 0.10 in., respectively. S_5, rectangular detector slit 0.001 in.×0.963 in.; long dimension perpendicular to plane of drawing. A, ionization chamber forming lower section of counter assembly shown in Ref. 1. DP, 400 liter/sec oil diffusion pump. B_1 and B_2, bellows-type vacuum joints constrained by external gimbals. B_1 is used to align apertures S_1 and S_3 with direction of primary beam incident on S_1 from the left. B_2 is used for mechanically sweeping detector slit S_5 across the electrostatically analyzed set of particle beams emergent to the right from D_2. B_2 permits detector slit S_5 (and attached assemblies A and DP) to swing through a $\pm 20°$ arc in the plane of the drawing about center of rotation P_2.

exit of T_2 divided the different species of fast charged particles emergent from T_2 into separate beams. Each of these beams was measured by moving the entrance slit S_5 of the proportional counter detector across the beam while recording with single-channel pulse-height analyzers the integrated counts of "single" and "double" amplitude pulses. The single-amplitude pulses came from H^+ or H particles and the double-amplitude pulses came from H_2 or H_2^+. Counts occurred in both channels only when the neutral beam from primary H_2 neutrals was being scanned. In this case pulse-height discrimination was used to distinguish H from H_2 in the composite neutral beam emergent from the collision chamber. The geometry and properties of the proportional counter were discussed thoroughly in Ref. 1. A 256-channel pulse-height analyzer was used in setting the pulse-height acceptance limits of the single-channel analyzers.

A refinement of the original apparatus[1] was the addition of a servo mechanism to drive the counter entrance slit at a speed proportional to the primary ion beam current. This system greatly reduced errors due to beam current fluctuations. The servo drive signal was derived in the neutral beam measurements from a Faraday cup C_2 surrounding the entrance of chamber T_2 into which the unconverted ion beam emergent from T_1 was directed. In all cases only a small fraction of the beam entering T_1 was neutralized and all unconverted ions were received by the Faraday cup. High stability of the neutralizing chamber pressure was obtained with a specially designed gas leak.[11] Constancy of this pressure insured that the neutral beam entering T_1 was exactly proportional to the servo drive signal once the leak was set.

[11] D. L. Allensworth, Rev. Sci. Instr. **34**, 448 (1963).

CROSS-SECTION DETERMINATION

Cross sections were determined from the formula

$$\sigma_i(j)=I_i/I_j nd, \tag{1}$$

where $\sigma_i(j)$ is the cross section for production of secondary particles of type i by primaries of type j, I_j is the current of primary particles of type j, I_i is the current of secondary particles of type i, and nd is the equivalent number of gas molecules in the collision chamber per cm^2 of target area normal to the beam direction.

Because molecular flow conditions were present in the collision chamber the following relation holds

$$nd=\alpha p, \tag{2}$$

where p is the collision chamber pressure gage reading and α is a calibration constant having a fixed value for a given target gas and a given statistical distribution of incident-particle paths through the collision chamber. It is assumed that the distribution of ray paths is independent of the type and energy of primary beam used in these experiments.

With the further assumption that

$$N_i/N_j=I_i/I_j, \tag{3}$$

where N_i is the number of counts recorded while the detector is scanned across the type i secondary beam and N_j is the number of counts recorded while the detector is scanned across the type j primary particle beam, Eqs. (1)–(3) yield the following cross-section formula:

$$\sigma_i(j)=(N_i/N_j)(1/\alpha p). \tag{4}$$

Secondary particles produced at the edges of the entrance slit to chamber T_2 or "spurious secondaries" which are present in the incident beam entering the collision chamber are not dependent on the collision chamber pressure p. Either of these effects or the presence in T_2 of a residual gas or vapor having a different cross section than the target gas result in failure of Eq. (4) to give a correct cross section. All three sources of error can be eliminated by plotting N_i versus p and by using the slope $\Delta N_i/\Delta p$ of this curve in place of N_i/p in evaluating Eq. (4). This procedure was used in every cross-section determination of the present work.

To summarize, the general working cross-section formula is

$$\sigma_i(j)=(1/\alpha N_j)(\Delta N_i/\Delta p). \quad (5)$$

CALIBRATION

The calibration of the apparatus consisted of determining a single value of the gas-dependent constant α of Eq. (5) since all measurements were made with H_2 as the target gas. This constant was determined by measuring the conversion of protons to H atoms by electron capture in H_2 gas (reaction 10) and assuming the cross-section value 8.2×10^{-16} cm^2 at the calibration proton energy of 10 keV. The value of α was found to be constant within a range of $\pm5\%$ in several determinations made during the course of the work. The chief cause of variations in successive α determinations was beam current fluctuations. The servomechanism used to compensate for beam current variations in all of the other measurements herein reported could not be used for the calibration because when the H^+ beam current was made low enough that the primary beam could be counted directly at the output of T_2, the fringing portion of the beam entering Faraday cup C_2 was too weak to provide a monitoring signal to drive the servo properly. This difficulty was offset in the calibration by taking a large number of points on the N_i versus p curves.

The use of reaction 10 for calibration continues the practice begun during our earlier work of reducing all hydrogen target measurements to a common basis. Should the value assumed for this cross section prove to be in error in the future, all of our measurements can be corrected accordingly by applying the same multiplicative correction factor throughout.

EXPERIMENTAL CONDITIONS

Hydrogen gas at a pressure between 10^{-4} and 10^{-3} mm Hg was used as the neutralizing gas in all of the neutral beam measurements. These pressures were sufficiently low that less than 10% of the incident ions were neutralized. The residual gas pressure in the neutralizing chamber was about 10^{-5} mm Hg with the gas inlet valve closed and about 10^{-6} mm Hg with the bypass valve open for calibration measurements.

Hydrogen gas of 99.9% purity was used in the collision chamber as the target gas. The residual gas pressure in the main collision chamber was 5×10^{-7} mm Hg with the hydrogen inlet leak closed and was varied between 10^{-5} and 10^{-4} mm Hg in order to obtain

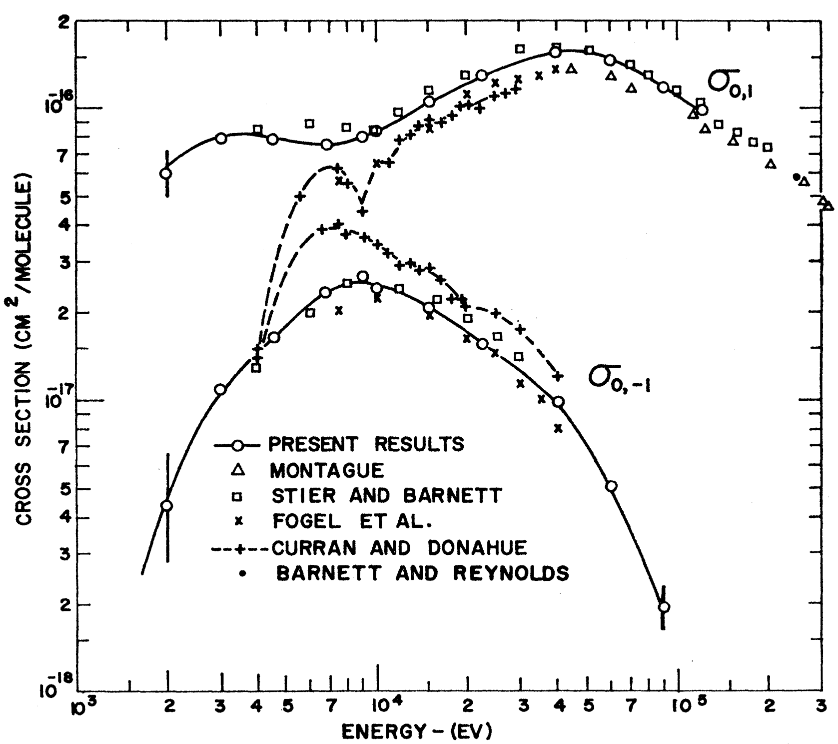

FIG. 2. Cross section $\sigma_{0,1}$ for conversion of primary H atoms to H^+ ions and cross section $\sigma_{0,-1}$ for conversion of primary H atoms to H^- ions. Present results are compared with previous data of Montague (Ref. 3), Stier and Barnett (Ref. 4), Barnett and Reynolds (Ref. 5), Fogel *et al.* (Refs. 6 and 7), and Curran and Donahue (Ref. 8).

the N_i versus p curves. The maximum fraction of incident particles which suffered either charge changing of dissociative collisions in the collision chamber was 0.7% and the maximum fraction of either the primary or secondary particles which underwent charge changing or dissociative collisions in the drift space between the collision chamber and the detector at the maximum drift space pressure of 10^{-6} mm Hg was about 0.07%. Under these conditions the attenuation of both the primary beam and secondary beams during traversal of the collision chamber and drift space could be ignored in evaluating the quantities N_i and N_j. Direct evidence of thin-target conditions was seen in the fact that all of the N_i versus p curves were linear within the statistical uncertainties of the particle counts. This uncertainty varied from 2 to 10%.

Ion beam currents entering chamber T_1 were generally of the order of 10^{-13} A throughout the data runs.

RESULTS

H Primaries

By permitting reaction 10 to occur in chamber T_1 and by applying a suitable deflection voltage to plate D_1 a beam of H atoms cleared of H^+ and H^- ions was directed into the collision chamber T_2. The fast secondaries H^+ and H^- emergent from T_2 due to reactions 8 and 9 were deflected by plates D_2 at angles of ± 3 deg from the unconverted H primary beam. Scans of the detector across all three beams at several energies indicated that a 1-deg scan was sufficient to receive essentially all of the particles emergent from the 4.4-deg-wide collision chamber exit aperture S_4. Consequently, 1-deg scans were used in all the $\sigma_{0,1}$ and $\sigma_{0,-1}$ measurements. For determinations of $\sigma_{0,1}$ the H^+ and H beams were scanned by the detector at several collision chamber pressures. Throughout these scans the H^+ beam emergent from chamber T_1 was collected at cup 2 and used as a servo drive signal. Calculation of the cross section $\sigma_{0,1}$ was then accomplished by the direct application of Eq. (5). Results are plotted in Fig. 2.

Except in the neighborhood of 10 keV the yield of H^- particles from reaction 9 was found to be so low that a large increase in the primary H beam was needed for accurate H^- yield determinations. In order to avoid correcting the recorded H counts for large dead-time losses at the required increased beam intensities, cup C_3 was moved into position to collect the H beam emergent from T_2 and a suitable positive bias was applied to the suppressor ring at the entrance to the cup to give a large secondary electron signal. This signal was then used to drive the servo while the H^+ and H^- beam were alternately scanned at several pressures to obtain plots of N_{H^+} and N_{H^-} versus pressure. The ratio $\sigma_{0,-1}/\sigma_{0,1}$ was then determined from the formula

$$\sigma_{0,-1}/\sigma_{0,1} = [\Delta N_{H^-}/\Delta p]/[\Delta N_{H^+}/\Delta p] \qquad (6)$$

and $\sigma_{0,-1}$ was determined by multiplying this ratio by the values of $\sigma_{0,1}$ from Fig. 2. The results for $\sigma_{0,-1}$ are shown also in Fig. 2.

Uncertainties in the experimental points are $\pm 5\%$ except for the points at 2 and 90 keV where larger uncertainties are indicated.

Previous measurements of $\sigma_{0,1}$ and $\sigma_{0,-1}$ are shown in Fig. 2 together with the present results. At all energies from 4 to 120 keV except in the vicinity of 6 keV our results appear to be consistent with the results of Stier and Barnett.[4] Agreement is excellent for both $\sigma_{0,1}$ and $\sigma_{0,-1}$.

In the energy range 40 to 120 keV our data points and those of Stier and Barnett for $\sigma_{0,1}$ fall about 15% above those of Montague.[3] Between 15 and 40 keV the results of all investigators scatter over a range of $\pm 20\%$ from the mean, but smooth curves drawn through the individual sets of data possess very nearly the same shape. It seems likely, therefore, that the discrepancies in this region could be accounted for by uncertainties in collision chamber pressure determinations.

Schwirtzke[9] has determined a quantity he calls $\sigma_{0,1}$ which we believe is actually $\sigma_{0,1}+\sigma_{0,-1}$. The Schwirtzke result, thus interpreted, has been compared with values of $(\sigma_{0,1}+\sigma_{0,-1})$ calculated from our data and is found to agree within $\pm 15\%$ over the range 10–50 keV.

Below 10 keV the experimental values of $\sigma_{0,1}$ fall into two divergent groups with relatively high values given by the present results and those of Stier and Barnett, and relatively low values given by Curran and Donahue[8] and by Fogel *et al.*[6,7] The Fogel measurements do not extend below 7 keV where an extremely serious departure sets in between the present "high" values and the "low" values of Curran and Donahue.

In an attempt to understand the drastic departure between the $\sigma_{0,1}$ results of Curran and Donahue and the $\sigma_{0,1}$ values of the present investigation below 7 keV we have hypothesized the presence of the well-known excited 2*s* metastable state in our H atom beam which was not completely quenched by the relatively low electric field used between deflection plates D_1. This proposal seemed worthy of investigation since the energy defects in the two reactions

$$H(1s)+H_2 \rightarrow H^+ + (H_2+e),$$
$$H(2s)+H_2 \rightarrow H^+ + (H_2+e)$$

(13.6 and 3.4 eV, respectively) are such that the latter should have a relatively high cross section. Thus even if the percentage of atoms in the 2*s* state were small, the effect on the weighted average value of $\sigma_{0,1}$ could be large.

According to a private communication,[12] the fields used by Curran and Donahue[8] were large enough to give complete quenching of the 2*s* metastable; however, deliberate steps were not taken in our measurements to suppress the 2*s* states completely. The fraction of 2*s*

[12] T. M. Donahue (verbal communication, 1963).

atoms surviving after passing through the deflection field at D_1 was calculated from the expression

$$\phi=\exp\left[-\int_0^b \nu(x)\,(dx/v)\right], \qquad (7)$$

where ϕ, the survival probability, is defined as the ratio of the 2*s* atom current leaving the D_1 deflection field region to that entering the D_1 deflection region from chamber T_1, $\nu(x)$ is the local decay rate of 2*s* atoms at distance x from slit S_2, v is the H atom velocity, and b is the length of path from S_2 to the end of the deflection plates. The quantity $\nu(x)$ was calculated from the formula $\nu(x)=A[E(x)]^2$ where E is the estimated electric field strength at distance x and A is a constant equal to 2780 sec^{-1} V^{-2} cm^2.[13] [Equation (7) is based on the assumption that the incremental fraction of 2*s* atoms decaying in time increment dt is equal to the product νdt where ν is an instantaneous decay rate given by the "static-field" formula quoted.]

For the set of points plotted in Fig. 2 the calculated 2*s* survival probabilities are given in Table I. The rather irregular variation of the survival probability is caused by the extreme sensitivity of this quantity to the deflection voltage coupled with the fact that no special attempt was made to choose deflection voltages which would lead to a regular variation of ϕ. In some cases, particularly at low energies, the survival probabilities were somewhat large; hence a subsidiary experiment was performed as a specific test of a possible 2*s* effect.

Two measurements of $\sigma_{0,1}$ were made at 4 keV (not plotted in Fig. 2) in which the deflection voltages used on plates D_1 were 85 and 25 V, respectively, and for which the survival probabilities were 0.02 and 0.71, respectively. The two results were $\sigma_{0,1}(85\text{ V})=7.92\pm0.4$ and $\sigma_{0,1}(25\text{ V})=8.28\pm0.5$, indicating that the maximum increase in the cross section $\sigma_{0,1}$ due to 2*s* atoms would be about 20%. Therefore, a variable population of the 2*s* level does not seem to afford an explanation for the discrepancy with the Curran-Donahue results.

TABLE I. Calculated survival probabilities [ϕ, Eq. (7)] of 2*s* metastable atoms traversing deflection plates D_1 in the $\sigma_{0,1}$ measurements as a function of H atom energy.

Energy keV	Survival probability
2	0.145
3	0.206
4.5	0.276
6.8	0.095
9	0.270
10	0.575
15	0.056
22.5	0.10
40	0.0057
66	0.4×10^{-4}
120	10^{-3}

[13] H. Bethe and E. Salpeter, *Handbuch der Physik*, edited by S. Flügge (Springer-Verlag, Berlin, Germany, 1957), Vol. XXXV, p. 373.

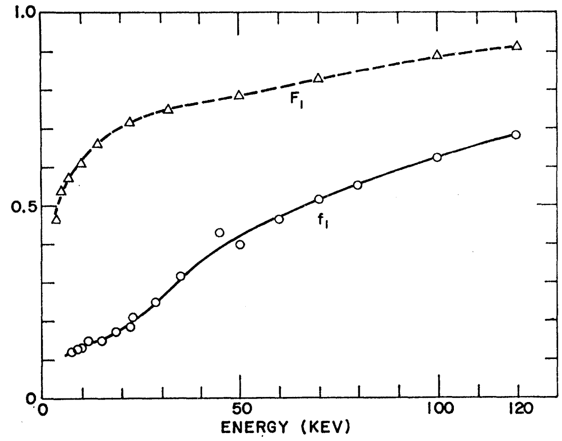

FIG. 3. Ratio $f_1=N_H/(N_H+N_{H_2})$, where N_H and N_{H_2} are, respectively, the fluxes of H atoms and H_2 molecules in the composite neutral beam entering collision chamber T_2 during the H_2 primary measurements. Ratio $F_1=\sigma_H/(\sigma_H+\sigma_{H_2})$, where σ_H and σ_{H_2} are, respectively, the cross sections for production of fast H and H_2 secondaries in collisions of fast H_2^+ ions with H_2 molecules. F_1 is calculated from the experimental data of Ref. 1.

H_2 Primaries

A composite neutral beam comprising fast H_2 molecules and H atoms was formed by passing magnetically analyzed H_2^+ ions into the neutralizing chamber. Fast H_2 and H neutrals produced in reactions 5, 6, and 7 emerged from the neutralizing chamber and entered the collision chamber while the emergent H_2^+ and H^+ ions were deflected out of the beam by deflector D_1.

The intensity and composition of the neutral beam emergent from T_2 was determined by making detector scans 1 deg wide. These scans were shown to be ample to cover the entire beam by trial runs at various widths. (The maximum angle of divergence of a primary neutral from the collision chamber axis was 0.38 deg as determined by the sizes of apertures S_2 and S_3.) Figure 3 shows the composition of the composite neutral beam emergent from T_2 as a function of the H_2 beam energy. The composition is described by the quantity

$$f_1=N_H/[N_{H_2}+N_H], \qquad (8)$$

where N_H and N_{H_2} are, respectively, the H and H_2 counts recorded in a scan of the neutral beam. It may be seen that the composition varies considerably with beam energy and follows a form quite different from the function F_1 given by

$$F_1=\sigma_H/[\sigma_H+\sigma_{H_2}], \qquad (9)$$

where σ_H and σ_{H_2} are, respectively, the production cross sections for H and H_2 secondaries in the reactions 5–7 calculated from the data of Ref. 1. This difference between f_1 and F_1 results from the small solid angle

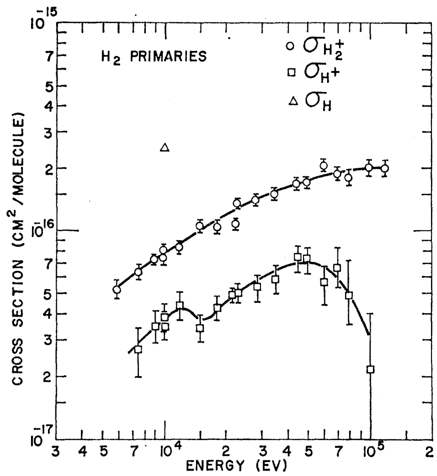

FIG. 4. Cross sections for conversion of fast H_2 molecules into fast secondaries H^+, H_2^+, and H in collisions with H_2 molecules. σ_{H^+}, $\sigma_{H_2^+}$, and σ_H are, respectively, the production cross sections of the secondaries H^+, H_2^+, and H.

subtended by aperture S_3 at the neutralizing chamber coupled with the fact that the H_2 molecules have a more strongly forward-peaked differential angular distribution than do the H dissociation products.

Because of the very narrow angular spread of the H_2 beam and the small size of apertures S_1 and S_3, it was necessary to carefully align the S_1–S_3 axis in order to achieve a minimum value of f_1 needed for optimum H_2 measurement accuracy. Owing to unexplained slight differences in the direction of the H_2^+ beam entering S_1 for various energies, care was taken to achieve good alignment at every accelerator energy. The slight departure of the point at 45 keV from the smooth curve f_1 probably resulted from misalignment which slightly favored H atoms at this energy.

To determine the cross sections for H_2^+ and H^+ production from H_2 primaries, a deflection voltage was applied to plates D_2 which deflected the secondary H_2^+ beam 3 deg from the main axis and the H^+ beam 6 deg. The neutral beam and the H_2^+ and H^+ beams were scanned repeatedly at several collision chamber pressures, providing curves of $N_{H_2^+}$ versus p and N_{H^+} versus p and values of N_H and N_{H_2}. Scan widths were adjusted to achieve complete collection of the H^+ and H_2^+ secondaries at each energy. One-deg scans sufficed for H_2^+ at all energies and 2-deg scans were sufficient for H^+ at all but the lowest energies. Below 10 keV the full 4.4-deg scans were used and considered to be adequate. The cross section $\sigma_{H_2^+}$ for H_2^+ production was straightforwardly determined from the formula

$$\sigma_{H_2^+}=\frac{1}{\alpha}\frac{1}{N_{H_2}}\frac{\Delta N_{H_2^+}}{\Delta p} \tag{10}$$

obtained from Eq. (5) with appropriate substitutions.

Cross section σ_{H^+} for production of H^+ by H_2 primaries was determined by first calculating

$$\sigma_T=\frac{1}{\alpha}\frac{1}{(N_{H_2}+N_H)}\frac{\Delta N_{H^+}}{\Delta p}, \tag{11}$$

which represents the average cross section for H^+ production by both the H_2 molecules and H atoms in the primary beam. The cross section σ_{H^+} for H^+ production by the H_2 primaries alone and the cross section $\sigma_{0,1}$ for production of H^+ by H primaries alone are related to σ_T by the equation

$$\sigma_T=f_1\sigma_{0,1}+f_2\sigma_{H^+};\quad f_2=1-f_1, \tag{12}$$

which can be rearranged in the form

$$\sigma_{H^+}=\sigma_T/f_2-\sigma_{0,1}f_1/f_2. \tag{13}$$

All the quantities on the right of Eq. (13) are known from the measurements described. Values of $\sigma_{0,1}$ were taken from the present data shown on Fig. 2 using the cross section for H atoms of one-half the H_2 beam energy. Deduction of correct values of σ_{H^+} by use of this formula rests on the assumption that the H atoms produced by H_2^+ dissociation in the neutralizing chamber have the same electron loss cross section as H atoms produced by proton neutralization in the neutralizing chamber.

The results of the σ_{H^+} and $\sigma_{H_2^+}$ measurements are shown in Fig. 4. The uncertainties associated with counting statistics (standard deviations) are indicated by the error flags. These are believed to dominate all other sources of error. The relatively large uncertainties in the σ_{H^+} values are associated with the relatively

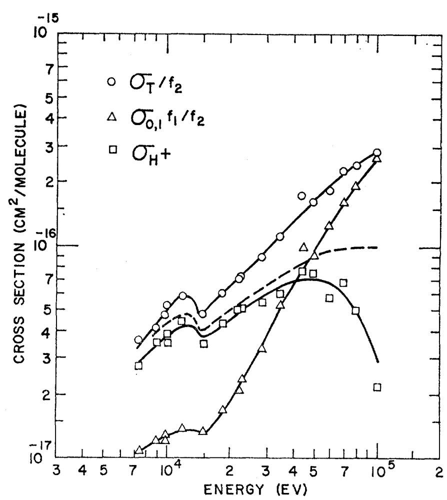

FIG. 5. Cross section σ_{H^+} for fast proton production by H_2 primaries and the two quantities σ_T/f_2 and $\sigma_{0,1}f_1/f_2$ [see Eq. (13)] which enter into the calculation of σ_{H^+}. The small difference between the upper curves at the higher energies leads to the large statistical uncertainties in σ_{H^+} at high energies. Dashed curve is the curve for σ_{H^+} obtained by using the lower values of $\sigma_{0,1}$ given by Curran and Donahue (Ref. 8) and Fogel (Ref. 7) instead of the $\sigma_{0,1}$ values from the present work in evaluating Eq. (13).

small cross sections as well as the fact that σ_{H^+} is a difference between two quantities [Eq. (13)], each of which has associated statistical errors. This difference became quite small at high energies, leading to quite large percentage uncertainties. The two terms appearing on the right-hand side of Eq. (13) and the difference σ_{H^+} are plotted in Fig. 5 to show clearly the relative magnitude of the quantities as they occurred in the σ_{H^+} determinations.

The effect on σ_{H^+} of assuming the lower set of $\sigma_{0,1}$ values given by Curran and Donahue (4- to 40-keV H atom energy) and Fogel (40- to 50- keV H atom energy) is indicated by the dashed curve in Fig. 5. This curve is believed to represent a less reliable estimate of σ_{H^+} than the solid curve since the "low" values of $\sigma_{0,1}$ used in calculating the dashed curve may have resulted from calibration disparities which were eliminated in the present set of measurements by our use of a common basis of calibration in the $\sigma_{0,1}$ and σ_T measurements.

The cross section σ_H for fast H atom production in reactions 1 and 3 could not be determined accurately because the high flux of H atoms in the primary neutral beam tended to mask the production of secondary H atoms at small angles. However, an estimate of σ_H was made at 10 keV as follows. Careful measurements of the angular distribution of fast H atoms emergent from the collision chamber were made at two collision chamber pressures with results shown in Fig. 6. At angles greater than $\frac{1}{2}$ deg a very distinct pressure-dependent H atom component is present corresponding to an H atom production cross section of 1.25×10^{-16} cm². The portion of this cross section due to H_2 dissociation is estimated as 1.17×10^{-16} cm² by subtracting the calculated amount expected from Coulomb scattering of H atoms in the primary beam. By making a linear extrapolation of the large-angle H atom distributions to zero angle, the estimated ratio of total H atom production to production outside $\frac{1}{2}$ deg was found to be 2.14, giving a final estimate of 2.5×10^{-16} cm² for the value of σ_H.

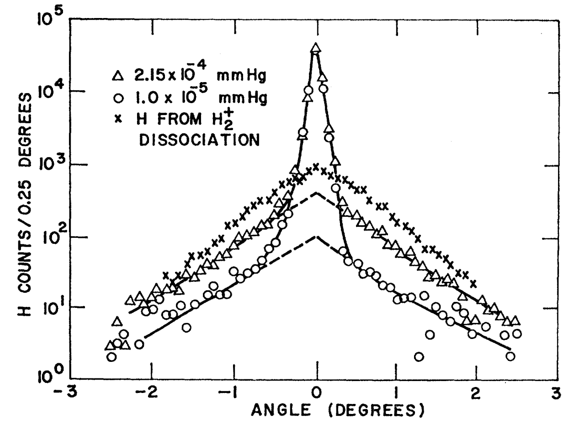

FIG. 6. Angular distribution of fast H atoms measured in order to estimate σ_H the cross section for production of fast H atoms from H_2 primaries. The large peak in the center is due principally to H atoms present in the primary beam and, consequently, shows no dependence on collision chamber pressure over the indicated pressure range 1.0×10^{-5} to 2.15×10^{-4} mm Hg. Dashed lines show extrapolations used in estimating the small-angle production of H atoms due to H_2 dissociation. Crosses indicate angular distribution of H atoms from H_2^+ dissociation in collision with H_2. All distributions are for 10 keV primaries and were obtained with a long slit (S_5) as the detector window. The distributions are, therefore, not the same as "differential angular distribution" in the usual sense of the term.

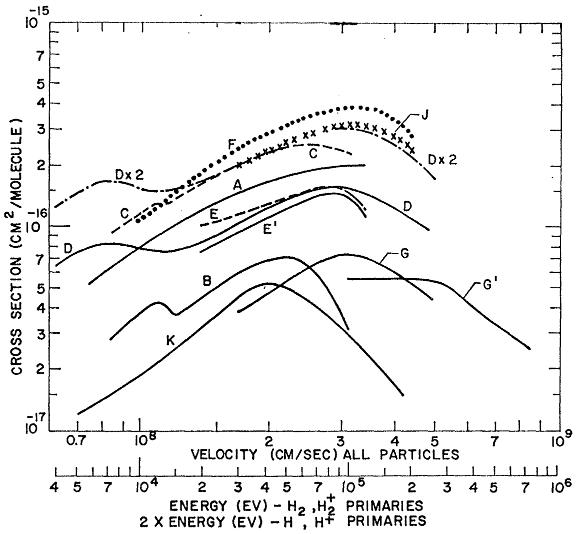

FIG. 7. Curve A: $\sigma_{H_2^+}$ the cross section for conversion of fast H_2 molecules to H_2^+ ions from Fig. 4. Curve B: σ_{H^+} the cross section for conversion of fast H_2 molecules to H^+ ions from Fig. 4. Curve C gives the sum of σ_{H^+} and $\sigma_{H_2^+}$ which equals the total cross section for electron loss from fast H_2 molecules. Curves D and D×2 are, respectively, 1 and 2 times the cross section $\sigma_{0,1}$ for electron loss from H atoms from Fig. 2. Curve E: ionization of H_2 by H primaries, including $\sigma_{1,-1}$ the ion production due to electron capture by the primary ions from Schwirtzke (Ref. 9). Curve E′: curve E minus $\sigma_{1,-1}$ from Fig. 2. Curve F: cross section for free electron production in $H_2^+ + H_2$ collisions from Afrosimov (Ref. 15). Curve G and G′ are, respectively, the results of Guidini (Ref. 16) and Sweetman (Ref. 2) for electron loss from H_2^+ ions in collision with H_2. Curve J: curve F with curve G subtracted to give cross section for electron removal from H_2 when struck by H_2^+. Curve K: cross section for production of slow H^+ ions in collision of H_2^+ with H_2 from Afrosimov (Ref. 15). A portion of curve D×2 between abscissa values 1.5 and 3×10^8 cm/sec was deliberately left out to avoid confusion with curve J.

The use of the linear extrapolation in estimating the small-angle H atom yield could not be rigorously justified, but seemed reasonable in view of the shape of the angular distribution of H atoms from H_2^+ primaries obtained with the same apparatus and shown superimposed in Fig. 6 for comparison.

DISCUSSION

No directly applicable theoretical calculations are available for comparison with the present experimental results; however, it is instructive to compare the previously available cross section data on several different hydrogen atom and molecule collisions with the new data on H_2+H_2 collisions. To facilitate such a comparison, a number of cross section vs velocity curves have been compiled in Fig. 7.

Curves A and B are the present $\sigma_{H_2^+}$ and σ_{H^+} results from Fig. 4. Curve C is the sum of $\sigma_{H_2^+}$ and σ_{H^+} which represents the total cross section for electron loss from the H_2 projectile in an H_2+H_2 collision. Curves D and D$\times$2 are, respectively, the cross section $\sigma_{0,1}$ for electron loss from H atoms and $\sigma_{0,1}$ multiplied by two. It may be seen from a comparison of curves C and D$\times$2 that the H_2 molecule does not behave as two separate H atoms in regard to electron loss except in a very narrow velocity range centered at about 1.7×10^8 cm/sec. The question of the similarity of H_2 to two separate H atoms in the somewhat different situation of proton charge exchange has been discussed by Tuan and Gerjuoy.[14] They conclude that there are important interference effects between the capture amplitudes from two interacting H atoms which can make the capture cross section quite dependent upon nuclear separation. The above noted disparity between curves C and D$\times$2 does not seem surprising in view of the possibility of analagous interference effects in the electron loss process. Curve E is the cross section given by Schwirtzke[9] for ionization of H_2 by H atoms while curve E′ is the same cross section with $\sigma_{1,-1}$ subtracted to eliminate the ionization contribution due to electron capture by the H primaries. It may be seen that curve C lies about a factor of 2 above curve E′, indicating that H_2 molecules are about twice as effective in removing electrons from H_2 molecules as are H atoms of the same velocity.

Curve F is the cross section for slow electron production in collisions of H_2^+ and H_2 as determined by Afrosimov *et al.*,[15] and curves G and G′ are, respectively, the results of Guidini[16] and Sweetman[2] for electron loss from fast H_2^+ ions in collisions with H_2. Curve J, the difference between curves F and G, represents the ionization of H_2 by H_2^+, not counting loss of electrons from the H_2^+ primaries. In the velocity range 1.7 to 2.2×10^8 cm/sec, curve J lies quite close to curve C, indicating that H_2^+ and H_2 are roughly equivalent in their power to remove electrons from H_2.[17] However, at 3×10^8 cm/sec there appears to be a real difference of about 50% between the two cross sections.

The cross section for removal of one electron from H_2 to form H_2^+ (curve A) is about three times larger than the cross section for removal of an electron from H_2^+ (curve G). This large difference seems reasonable since the first ionization potential of H_2 is 15 eV while the ionization potential of H_2^+ is 30 eV, indicating that the second electron is much more strongly bound than the first.

Curve K is the cross section for slow proton production in collisions of fast H_2^+ with H_2. This curve lies somewhat below curve B, indicating that the fast primary in H_2+H_2 collisions converts to H^+ with a slightly higher probability than the target particle in $H_2^++H_2$ collisions.

One of the more interesting results of this study is that the fast H atom yield from the pair H_2+H_2, measured at 10 keV, is only $\frac{1}{3}$ as great as the yield of fast H atoms from the pair $H_2^++H_2$ from Ref. 1. This may perhaps be explained by the fact that the lowest repulsive state of H_2 is the triplet state $1^3\Sigma_u$ which can only be reached from the ground state of H_2 by a spin flip or by electron exchange. Both of these processes are theoretically very unlikely compared with the simple near resonant process of electron transfer from an H_2 molecule to an H_2^+ ion, placing the newly formed molecule in a $1\,^3\Sigma_u$ repulsive state.

It is quite probable that the H_2 molecules which form the primary beam in our H_2 primary measurements (Fig. 4) are not in their ground vibrational states. This follows from the fact that the H_2^+ ion has a nuclear potential minimum at a nuclear spacing somewhat larger than that of the H_2 molecule. This has the effect of causing the H_2^+ ions to be formed preferentially in their third or fourth vibrational quantum level in which the vibrational excursion of nuclear spacing is quite large.[18] When the H_2^+ ions are subsequently converted back to H_2 by electron capture, the molecule may therefore be forced into very high vibrational levels. The degree of influence that vibrational excitation exerts on the H_2 ionization and dissociation cross sections has not yet been determined. Some evidence exists, however, of a dependence of H_2^+ dissociation cross sections on vibrational excitation.[1,19,20] Recent calculations[21] have shown a strong vibrational dependence of ionization of H_2^+ ions by electron impact.

ACKNOWLEDGMENT

The author is indebted to D. L. Allensworth for performing with skill and patience all of the hard labor connected with apparatus design, accelerator operation, and cross section data taking. The work was also aided by numerous stimulating and informative discussions with T. A. Green and J. M. Peek.

[14] T. F. Tuan and E. Gerjuoy, Phys. Rev. **117**, 756 (1960).
[15] V. V. Afrosimov, R. N. Ilin, and N. V. Fedorenko, Zh. Eksperim. i Teor. Fiz. **34**, 1398 (1958) [English transl.: Soviet Phys.—JETP **7**, 968 (1958)].
[16] J. Guidini, Compt. Rend. **253**, 829 (1961).
[17] Here we compare electron loss from the *target* H_2 molecule in the $H_2^++H_2$ collision with electron loss from the projectile in the H_2+H_2 collision.
[18] P. Marmet and T. Kerwin, Can. J. Phys. **38**, 972 (1960).
[19] A. C. Riviere and D. R. Sweetman, Proc. Phys. Soc. (London) **78**, 1215 (1961).
[20] C. F. Barnett and J. A. Ray, Third International Conference on Ionization Phenomena in Gases, 1963, University College, London (unpublished).
[21] J. M. Peek, Sixteenth Annual Gaseous Electronics Conference, 1963, Pittsburgh, Pennsylvania (unpublished).